C–H , O Hydrogen bonded multi-point recognition in molecular assemblies of dibenzylidene ketones and 1,3,5-trinitrobenzenes

Kumar Biradha,[a] Ashwini Nangia,*[a] Gautam R. Desiraju,*[a] C. J. Carrell[b] and H. L. Carrell*[b]

[a]*School of Chemistry, University of Hyderabad, Hyderabad 500 046, India*

[b]*The Institute for Cancer Research, Fox Chase Cancer Center, 7701 Burholme Avenue, Philadelphia, PA 19111, USA*

Dibenzylideneacetone **1a**, 2,5-dibenzylidenecyclopentanone **1b**, 2,6-dibenzylidenecyclohexanone **1c** and 2,5-dibenzylidenecyclopent-3-enone **1d** form crystalline stoichiometric complexes with 1,3,5-trinitrobenzene **2a**, picryl chloride **2b** and picric acid **2c**. The structures of these complexes are mediated by multi-point C–H , O hydrogen bonds. Some of these patterns of molecular recognition also contain stronger O–H , O hydrogen bonds. The C–H , O hydrogen bonds within these multi-point supramolecular synthons are generally shorter and more linear than the other C–H , O hydrogen bonds found in these complexes.

The assembly of molecules into nanosize aggregates has emerged as a major endeavour in modern chemistry.[1] It has been recognised that nanoscale systems represent a meeting point of the chiselling down by technologists of macrosize precursors and of the building up by chemists from molecular size precursors. Supramolecular systems formed by self-organisation principles are good examples of nanostructures. Supramolecular chemistry emphasises the collective properties of molecules and in this regard, the physical and chemical properties of molecular aggregates are often significantly different from those of the constituent molecules.[2]

A crystal is a supermolecule *par excellence*[3] and the recognition patterns that are formed in crystals may be termed supramolecular synthons if a crystal is viewed as a retrosynthetic target.[4] Crystal engineering, the premeditated assembly of molecules in the solid state, then becomes the supramolecular equivalent of organic synthesis and accordingly, a supramolecular synthon may be defined as a structural unit within a supermolecule which can be formed and/or assembled by known or conceivable synthetic operations involving intermolecular interactions. Crystal engineering with conventional (or strong) O–H , O and N–H , O hydrogen bonds may appear sufficiently reliable, but it is in reality incomplete if weak intermolecular interactions are not considered.[5] The advantage of using weak intermolecular interactions in crystal engineering is that the repertoire of compounds that can be used to construct supramolecular motifs and patterns is significantly increased.

Among the weak intermolecular interactions, C–H , O hydrogen bonds have attracted considerable attention. The ability of the C–H group to form various types of hydrogen bonds, such as C–H , O,[6a–c] C–H , N,[6d] C–H , F[6e] and C–H , M,[6f] is well-established and is comparable to that of the N–H and O–H groups. Cambridge Structural Database (CSD) studies on several aspects of C–H , O hydrogen bonds have resulted in a better understanding of the nature of these interactions[7] and this in turn has led to the utilisation of these interactions in the construction of supramolecular synthons through a consideration of the complementarity of functional groups.[8] Recently, we have shown that the C–H group in organometallic cluster compounds also forms C–H , O hydrogen bonds with the CO ligand and that the stability of these interactions depends on the basicity of the CO ligand.[9] These studies also reveal that C–H , O=C hydrogen bonds are directional with the preferred C=O , H angle being around 140°. All these studies suggest that C–H , O hydrogen bonds show properties similar to those of strong hydrogen bonds. To summarise, C–H , O hydrogen bonds can be used quite efficiently in the design of supramolecular synthons and crystal structures. However, owing to the inherent weakness of these interactions, multi-point recognition rather than single-point recognition is the preferred strategy.

Here we aim to design and analyse the robustness of the three-point C–H , O recognition synthon **I** which is a mimic of the well-known synthon **II** that is constructed purely with strong hydrogen bonds. For this purpose, the crystal structures of complexes **3a–g** have been solved and analysed.[10] Synthon **I** is found to occur in complexes **3a–e** but not in **3f** and **3g**. The CSD was used to analyse the patterns observed in these structures and in some other a,b-unsaturated carbonyl compounds.

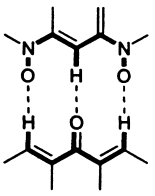

I

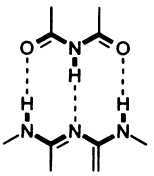

II

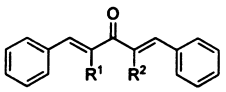

1

a $R^1 = R^2 = H$
b R^1-$R^2 = -CH_2CH_2-$
c R^1-$R^2 = -CH_2CH_2CH_2-$
d R^1-$R^2 = -CH{=}CH-$

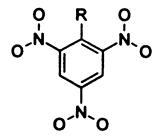

2

a R = H
b R = Cl
c R = OH

3

a 1a:2a (1:2)
b 1b:2a (1:2)
c 1c:2a (1:2)
d 1b:2b (1:2)
e 1d:2b (1:2)
f 1b:2c (1:1)
g 1a:2c (1:1)

Experimental

Preparation of materials

1,3,5-Trinitrobenzene **2a** was prepared in three steps from 2,4-dinitrotoluene. Nitration of 2,4-dinitrotoluene gave 2,4,6-

trinitrotoluene, which was oxidised with $K_2Cr_2O_7$ to provide 2,4,6-trinitrobenzoic acid.[11a,b] This was decarboxylated in the presence of NaOH to give compound **2a**.[11c] Picric acid **2c** was purchased and picryl chloride **2b** was prepared by the reaction of **2c** with $POCl_3$ and *N*,*N*-diethylaniline.[12] The dibenzylideneketones were prepared by the condensation reaction of 2 equiv. of benzaldehyde with 1 equiv. of the corresponding ketones. Compound **1d** was prepared by allylic dibromination of **1b** with *N*-bromosuccinimide (NBS)–CCl_4 followed by debromination with Zn–MeOH.[13] Pentacenedione was prepared by the condensation reaction of cyclohexane-1,4-dione and phthalaldehyde.[14]

Preparation of crystals

Yellow crystals of the 2:1 complex **3c** were obtained from an equimolar solution of **2a** and **1c** in 1:1 dichloromethane–hexane. Similarly, yellow crystals of the complexes **3d–g** were obtained from an equimolar solution of the molecular components in 1:1 chloroform–hexane. The preparation of complexes **3a** and **3b** has been described by us previously.[10]

X-Ray crystallographic studies

Data were collected for all the complexes on an Enraf-Nonius FAST area detector with a rotating anode X-ray source. The crystal structures of complexes **3a** and **3b** have been reported already[10] and only the essential features are given here. The crystal structures of complexes **3c–g** are presented here. The solution of the structures for all the complexes were carried out with the SHELXS86[15] program and the refinements were carried out with the SHELXL93 program.[16]

Complex **3c** crystallises in the triclinic space group P1. Most of the sample consisted of twinned crystals and the data were collected on a solitary untwinned sample. The solution for its crystal structure was obtained in the space group P1 since it failed to solve in P1; the structure was then refined in the space group P1. In complexes **3d** and **3e**, the dibenzylideneketone moiety and one of the nitro groups are disordered. It may be noted that this disorder could not be fully modelled in the refinements and that the attendant lack of precision in the atomic positions is unavoidable. This means that the finer details of the hydrogen bonding cannot be discussed in detail. However, these structures have been included here for the sake of completeness. All the non H-atoms were refined anisotropically. All the H-atoms, except in complex **3f**, were located from difference Fourier maps and refined isotropically in the final stages of the refinement because this is a study of the C–H , O hydrogen bonds. The hydrogen atoms in complex **3f** were fixed geometrically and refined with the riding model. Salient crystallographic information for the complexes in this study is given in Table 1.†

CSD studies

Data were retrieved from the CSD (ver. 5.08).[17] Screens −28, 34, 85 and 88 were used to eliminate organometallic entries and unmatched chemical and crystallographic connectivities. Entries with *R*-factor greater than 0.10 and disordered structures were also excluded. A C–H , O geometry was considered a *bona fide* hydrogen bond when the C , O distance is less than 4.0 Å and the C–H , O angle is between 110 and 180°. Geometrical calculations were performed using QUEST3D-GSTAT, an automatic graphical non-bonded search program of the CSD.

† Atomic coordinates, thermal parameters, and bond lengths and angles have been deposited at the Cambridge Crystallographic Data Centre (CCDC). See Information for Authors, *J. Mater. Chem.*, 1997, Issue 1. Any request to the CCDC for this material should quote the full literature citation and the reference number 1145/32.

Results and Discussion

Synthon I in complexes of 2a

The choice of trinitrobenzene **2a** as one of the components to form the supramolecular synthon **I** is due to the high acidity of its aromatic C–H and the ability of nitro groups to form C–H , O hydrogen bonds. The choice of dibenzylideneketones as the second supramolecular component is made by matching complementary groups. Our earlier observation[18] that a,b-unsaturated carbonyl compounds form C–H , O hydrogen bonded patterns **III** and **IV** further strengthened our idea for the choice of dibenzylideneketones.

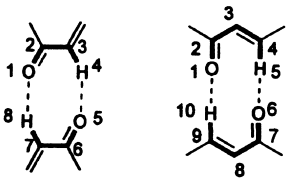

III **IV**

Compound **2a** forms a 2:1 crystalline complex **3a** with dibenzylideneketone **1a**. The expected synthon **I** is observed in **3a** and the overall crystal structure is fortified by additional C–H , O hydrogen bonds on the other side of the carbonyl group [Fig. 1(*a*)]. In order to avoid this alternate C–H , O hydrogen bonded pattern and also to assess the robustness of synthon **I**, we considered complexes of **2a** with **1b** and **1c** instead of **1a**. Compound **2a** also forms 2:1 crystalline complexes **3b** and **3c** with **1b** and **1c**, respectively [Fig. 1(*b*) and (*c*)]. Synthon **I** is found in both these complexes and the alternate C–H , O hydrogen bonded pattern which involves the hydrocarbon side of the molecule is found in complex **3b** but not in **3c**. The presence of the alternate motif on the hydrocarbon side in complexes of **1a** and **1b** is attributed to the higher acidity of vinylic and allylic C–H groups, respectively, which enables them to make the three-centre motif consisting of vinylic/allylic C–H, aromatic C–H and nitro oxygen atom. Curiously, the **1b** molecules in complex **3b** are disordered about a line that roughly bisects the molecular length because of the alternate C–H , O hydrogen bonded pattern. The observation that the occupancies of two orientations of **1b** in this complex are constrained by crystallographic symmetry to be 0.5 and 0.5 indicates that synthon **I** and the alternate C–H , O hydrogen bonded pattern are of comparable significance. The C–H , O hydrogen bond recognition pattern **V** is found in complexes **3b** and **3c** but not in **3a**. The presence of synthon **I** and pattern **V** in the complexes of **3b** and **3c** are shown in Fig. 1(*b*) and (*c*), respectively.

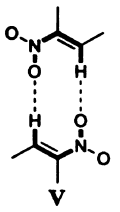

V

To analyse the C–H , O hydrogen bonds in the complexes of **2a**, plots of the C , O distances *versus* the C–H , O angles were obtained (Fig. 2). Circles, triangles and squares represent the C–H , O hydrogen bonds in complexes **3a**, **3b** and **3c** respectively. The C–H , O hydrogen bonds which are part of synthon **I** are shown as filled symbols. From this plot, one notes that the C–H , O hydrogen bonds within synthon **I** are shorter and more linear and that they constitute the essence of these crystal structures. This observation strengthens the idea that the significance of a C–H , O hydrogen bond increases if it is part of a multi-point synthon. The C–H , O hydrogen bonds of synthon **I** are strongest in complex **3b** but somewhat weaker in **3a**/**3c**.

Table 1 Crystallographic data of complexes **3a–g**

compound	**3a**	**3b**	**3c**	**3d**	**3e**	**3f**	**3g**
formula	$C_{29}H_{20}N_6O_{13}$	$C_{31}H_{22}N_6O_{12}$	$C_{64}H_{48}N_{12}O_{26}$	$C_{15.5}H_9ClN_3O_{6.5}$	$C_{15.5}H_9ClN_3O_{6.5}$	$C_{25}H_{19}N_3O_8$	$C_{23}H_{17}N_3O_8$
M	660.52	686.56	1641.34	376.71	376.71	489.43	463.40
crystal system	monoclinic	monoclinic	triclinic	monoclinic	monoclinic	orthorhombic	triclinic
space group	$P2_1$	$P2_1/c$	*P*1	$P2_1/n$	$P2_1/n$	$P2_12_12_1$	*P*1
a/Å	7.092(2)	7.493(2)	13.721(3)	7.481(2)	7.474(1)	5.915(2)	8.979(10)
b/Å	27.927(4)	27.384(6)	14.374(4)	15.140(4)	15.287(2)	9.722(6)	11.343(14)
c/Å	7.569(2)	7.491(2)	16.349(7)	14.394(7)	14.435(2)	39.097(4)	11.68(2)
a(°)			92.13(2)				76.63(6)
b(°)	96.67(2)	92.39(2)	102.67(2)	95.806(10)	96.42(2)		84.39(6)
c(°)			97.90(2)				68.84(9)
V/Å^3	1488.9(5)	1535.8(6)	3109(2)	1621.9(10)	1638.9(4)	2248(2)	1079(2)
T/K	293	293	120	293	293	293	293
Z	2	2	4	4	4	4	2
F(000)	680	708	1688	788	768	1016	480
D_c/g cm^{-3}	1.47	1.484	1.754	1.580	1.527	1.446	1.426
l/Å	0.7107	0.7107	0.7107	0.7107	0.7107	0.7107	0.7107
m/mm^{-1}	0.76	0.76	0.134	0.283	0.276	0.110	0.110
crystal size	0.23 × 0.31 × 0.30	0.22 × 0.25 × 0.33	0.1 × 0.1 × 0.2	0.24 × 0.22 × 0.35	0.26 × 0.20 × 0.38	0.20 × 0.15 × 0.3	0.15 × 0.20 × 0.3
radiation	Mo-Ka	Mo-Ka	Mo-Ka	Mo-Ka	Mo-Ka	Mo-Ka	Mo-Ka
h range (°)	1–27.5	1–27.5	2.56–28.69	2.69–25.35	2.94–27.30	2.162–28.96	2.37–23.50
h	−7 to 7	−7 to 7	0 to 11	0 to 9	0 to 9	0 to 8	0 to 10
k	0 to 34	0 to 33	−19 to 18	0 to 18	0 to 19	0 to 13	−11 to 12
l	0 to 8	0 to 8	−21 to 21	−17 to 17	−18 to 18	0 to 15	−12 to 13
total reflections	2931	3532	11741	2956	3571	3171	3062
unique reflections	1828	1328	6695	1634	2359	1867	1857
s-level	3	3	2	2	2	2	2
*R*1	0.038	0.048	0.049	0.08	0.16	0.04	0.05
*wR*2	0.041[a]	0.050[a]	0.12	0.23	0.47	0.12	0.11
min. electron density/e Å^{-3}	−0.19	−0.13	−0.404	0.238	−0.806	−0.204	−0.173
max. electron density/e Å^{-3}	0.13	0.13	1.826	0.282	0.524	0.163	0.195

[a] R_w values

Synthon I in complexes of 2b

To test the robustness of synthon **I** in the presence of other functional groups like Cl and OH, we have prepared complexes of **2b** with **1b** and **1d** and of **2c** with **1a** and **1b**. It is well known that **2c** forms stable complexes with various aromatic compounds through p–p interactions[19] and it has been used in crystal engineering experiments to design a three-point synthon **VI** that contains two C–H , O and one N–H , O hydrogen bonds.[20] From the examination of the crystal structures of pure **2b** and **2c**, it was found that the three nitro groups are coplanar with the aromatic ring in **2c** but not in **2b**. In **2b** the *ortho* nitro group which is not involved in intramolecular O–H , O hydrogen bond is out of the aromatic ring plane. Therefore, both **2b** and **2c** were expected to form complexes with dibenzylideneketones.

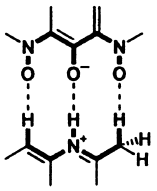

VI

Compound **2b** forms 2 : 1 crystalline complexes **3d** and **3e** with ketones **1b** and **1d**, respectively [Fig. 3(*a*) and (*b*)]. Even though compounds **1b** and **1d** are chemically different, they form isostructural complexes with **2b** due to the disorder in the dibenzylidene moiety. The presence of C–H , O hydrogen bonded synthon **I** in complexes **3d** and **3e** indicates that the Cl group does not interfere in the formation of **I**. These crystal structures are almost reminiscent of **3a**, **3b** and **3c** except that O , Cl interactions are formed as shown in pattern **VII**. The nitro group oxygen atoms which participate in **VII** are disordered. The disorder of molecule **1b** in these two complexes allows it to mimic a molecule of pentacenedione, as shown in Scheme 1. Therefore, it was anticipated that pentacenedione should cocrystallise with compound **2b** to yield **I**. However, this could not be realised experimentally because pentacenedione failed to cocrystallise with **2b** due to a mismatch of solubilities.

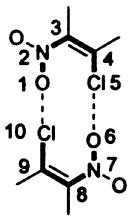

VII

Absence of synthon I in complexes of 2c

Compound **2c** forms 1 : 1 molecular complexes **3f** and **3g** with compounds **1b** and **1a**, respectively. In both complexes, the C–H , O hydrogen bonded synthon **I** is absent. Interestingly, in complex **3f** the O–H group forms an intermolecular hydrogen bond with the keto group of molecule **1b** (O , O, H , O, O–H , O; 2.90 and 2.06 Å, 123°). It also forms two C–H , O hydrogen bonds (C , O, H , O, C–H , O; 3.18 and 2.98 Å, 164° and 3.42 and 2.23 Å, 156°) to form a supermolecule of **1b** and **2c** that involves one O–H , O and two C–H , O hydrogen bonds [Fig. 4(*a*)]. The three-dimensional packing of these supermolecules is shown in Fig. 4(*b*). These results show that there is a limit to the robustness of synthon **I** in this family of crystal structures. Picric acid **2c** which contains a strongly hydrogen bonding OH group is capable of disrupting the recognition motif **I** of trinitrobenzenes with dibenzylideneketones.

In complex **3g**, the situation is entirely different from the other complexes in that there is no intermolecular O–H , O hydrogen bond with a keto group as in complex **3f**. Instead,

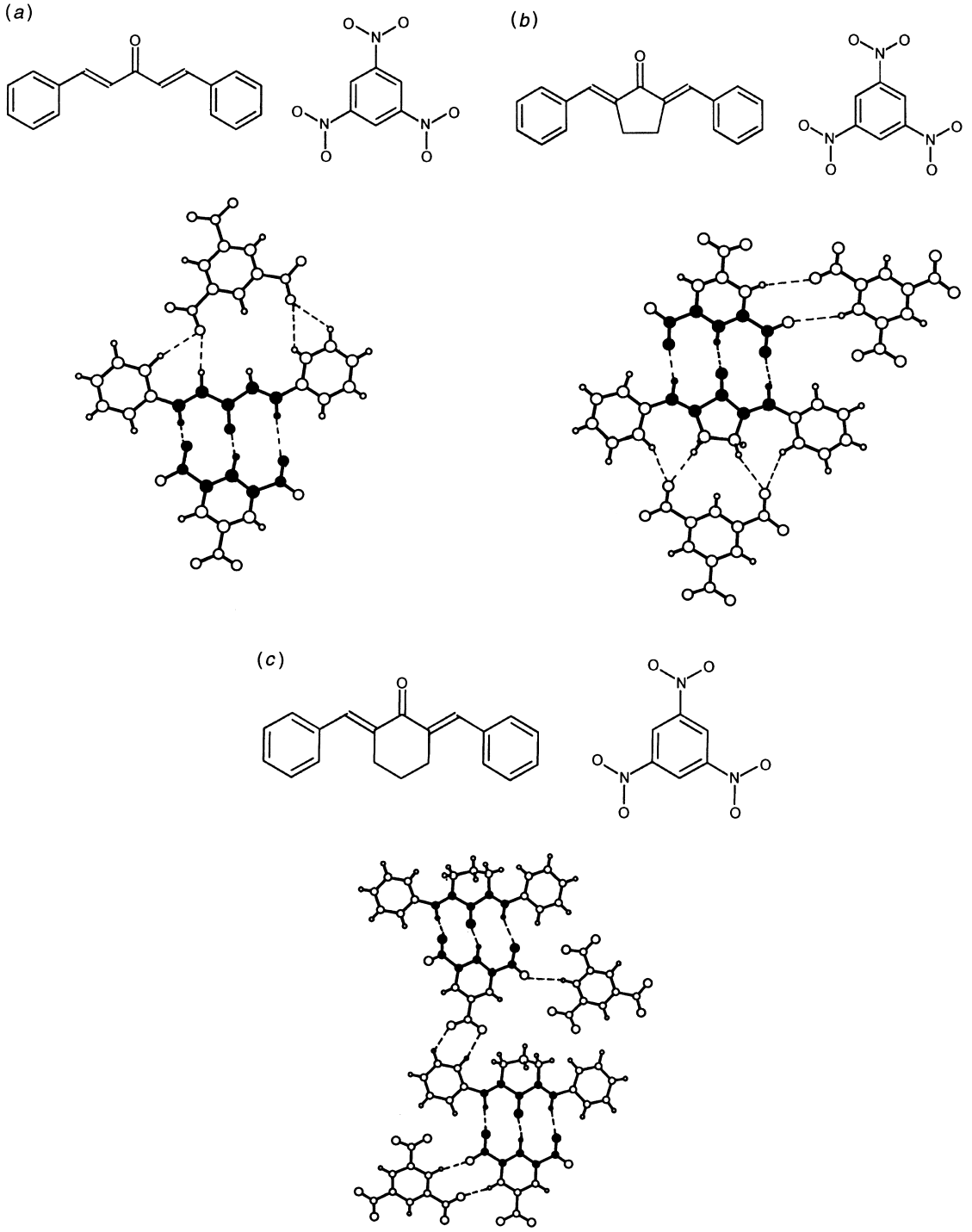

Fig. 1 (*a*) Crystal structure of complex **3a** (**1a**:**2a** in 1:2 ratio) to show synthon **I** (highlighted) and the alternate C–H , O hydrogen bonded patterns. (*b*) Crystal structure of complex **3b** (**1b**:**2a** in 1:2 ratio) to show synthons **I** and **V** and the alternate C–H , O hydrogen bonded patterns. (*c*) Crystal structure of complex **3c** (**1c**:**2a** in 1:2 ratio) to show synthons **I** and **V**.

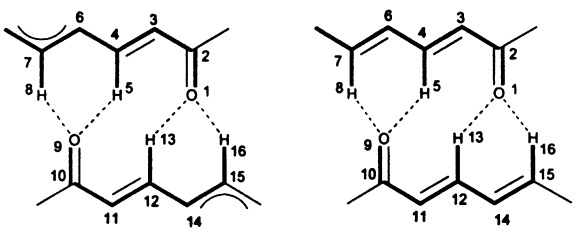

VIIIa **VIIIb**

one finds that centrosymmetric dimers of **1a** and **2c** are connected by C–H , O hydrogen bonds (Fig. 5). The dimer of **2c** is engaged in tandem hydrogen bonding[21] whereas that of **1a** is involved in C–H , O hydrogen bonded pattern **VIII**, which is another example of three-point recognition.

NIPMAT plots of complexes 3f and 3g

The differences in the packing of **3f** and **3g**, the two molecular complexes of **2c** with **1b** and **1a** respectively, have been examined by looking at their NIPMAT plots.[6c] A pictorial matrix is formed using the atoms of a molecular skeleton (A_1, A_2 , A_m , A_n) and the matrix element A_mA_n which is defined by the shortest intermolecular contact A_m , A_n and shown in terms of a grey scale. The shorter the contact, the greyer the square which represents that particular contact. This greyness is scaled at the bottom of the figure. The dark line in this scale indicates the sum of the van der Waals radii of any two atoms. If there are two different molecular skeletons (A_1, A_2 , A_m , A_n) and (B_1, B_2 , B_i , B_j) in the supramolecular structure, then their interactions are shown in four sections. The upper left and lower right rectangles indicate the A , B interactions while the lower left and upper right squares indicate A , A and B , B interactions. Hence, the plot obtained is a simultaneous visual representation of all the intermolecular interactions. Fig. 6(*a*) and (*b*) are the NIPMAT plots of complexes **3f** and **3g**, respectively. In Fig. 6(*b*), the overall greyness in the upper left and lower right rectangles, which represent the C–H , O interactions and stacking interactions between molecules **2c** and **1a**, is more when compared with the corresponding areas of Fig. 6(*a*) (**2c** and **1b**). This implies that in complex **3g** the C–H , O hydrogen bonds and stacking interactions dominate the packing of the crystal. In complex **3f**, compound **1b** has relatively less acidic sp^3 C–H groups compared to the sp^2 C–H moiety of **1a** and so the intermolecular O–H , O hydrogen bonds take the lead with the assistance of some weaker C–H , O bonds.

p–p Stacking interactions

The formation of 1 : 2 molecular complexes **3a–e** from solutions containing equimolar amounts of **1** and **2** can be justified by considering p–p stacking. A molecule of **1** contains two phenyl rings and can accommodate two molecules of **2**. It is well known that aryl groups prefer to interact in either an edge-to-face or an offset face-to-face orientation[22] and compound **2a** forms charge-transfer complexes with aromatic compounds.[23] Recently, compound **2a** has been used as a guest for chiral molecular tweezers through these interactions.[24] All the molecular complexes of **2a** and **2b** form these interactions with slightly offset stacking. Fig. 7 shows a superposition of these

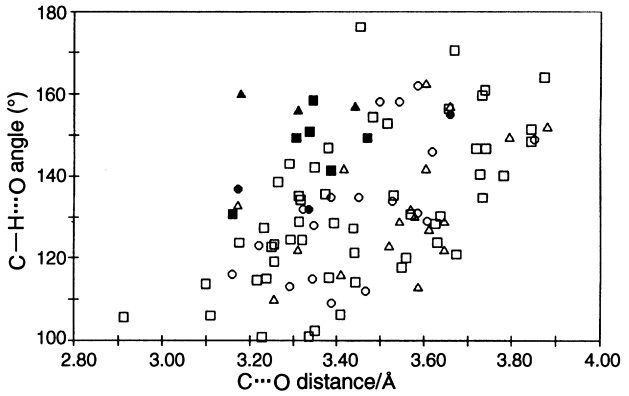

Fig. 2 Scatter plot of C–H , O interactions in the complexes (#) **3a**, (') **3b** and (%) **3c**. Filled symbols are the C–H , O hydrogen bonds that contribute to synthon **I**. Notice that all these filled symbols are in the strong hydrogen bonded region.

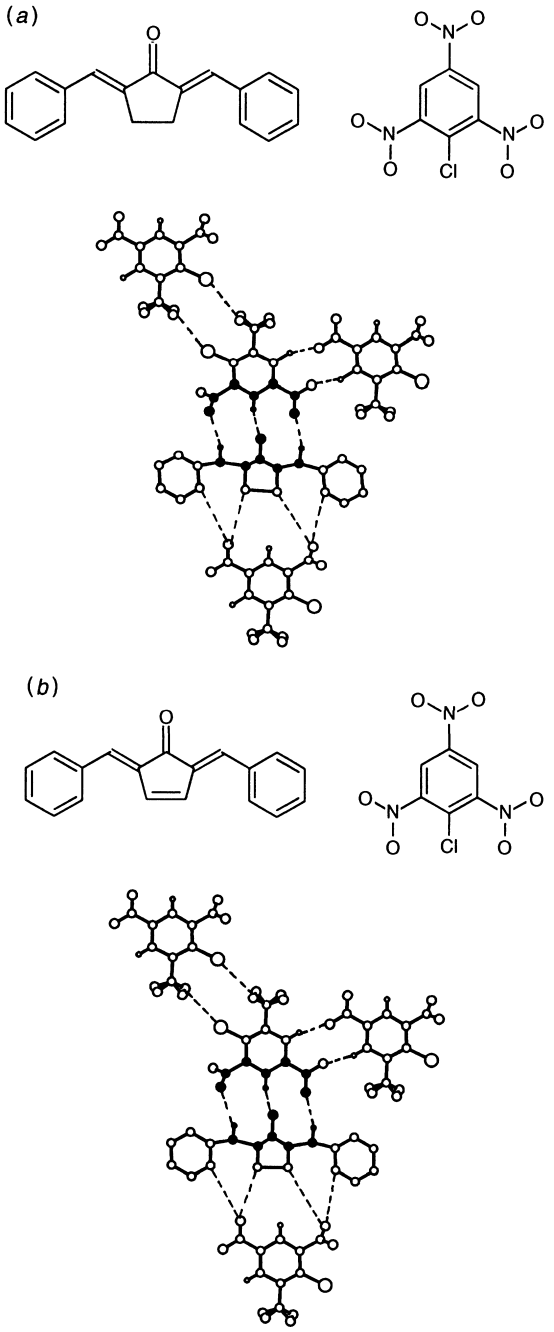

Fig. 3 (*a*) Crystal structure of **3d** (**1b** : **2b** in 1 : 2 ratio) to show synthons **I**, **V** and **VII**. (*b*) Crystal structure of **3e** (**1d** : **2b** in 1 : 2 ratio) to show synthons **I**, **V** and **VII**. Both disordered positions of the nitro group are shown for molecule **2b**.

interactions in the above complexes. The centroid to centroid distance and plane to plane angles in these complexes range from 3.64 to 4.83 Å and 0.81 to 10.4°. However, the stacking interactions are different in complexes **3f** and **3g**. Complex **3f** is stabilised by p–p and herringbone interactions [Fig. 4(*b*) and 7(*f*)] while complex **3g** is stabilised by p–p interactions alone [Fig. 7(*g*)]. The variation in the donor–acceptor ratios of complexes **3f** and **3g** when compared with that in **3a–e** is a consequence of the change in interactions between aromatic rings in these complexes.

CSD studies

The CSD was searched for the C–H , O hydrogen bonded patterns **III**, **IV** and **VIII** and O , Cl interaction **VII** to understand their nature and to ascertain their frequency of occurrence, which would indicate their robustness. There are

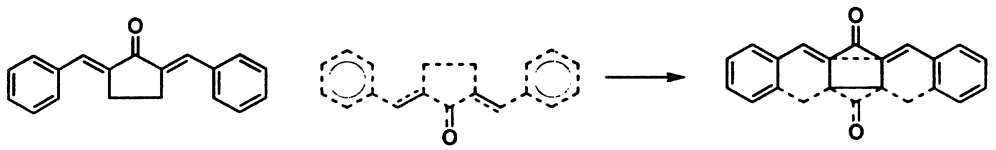

Scheme 1 Disorder of molecule **1b** and **1d** in complexes **3d** and **3e**

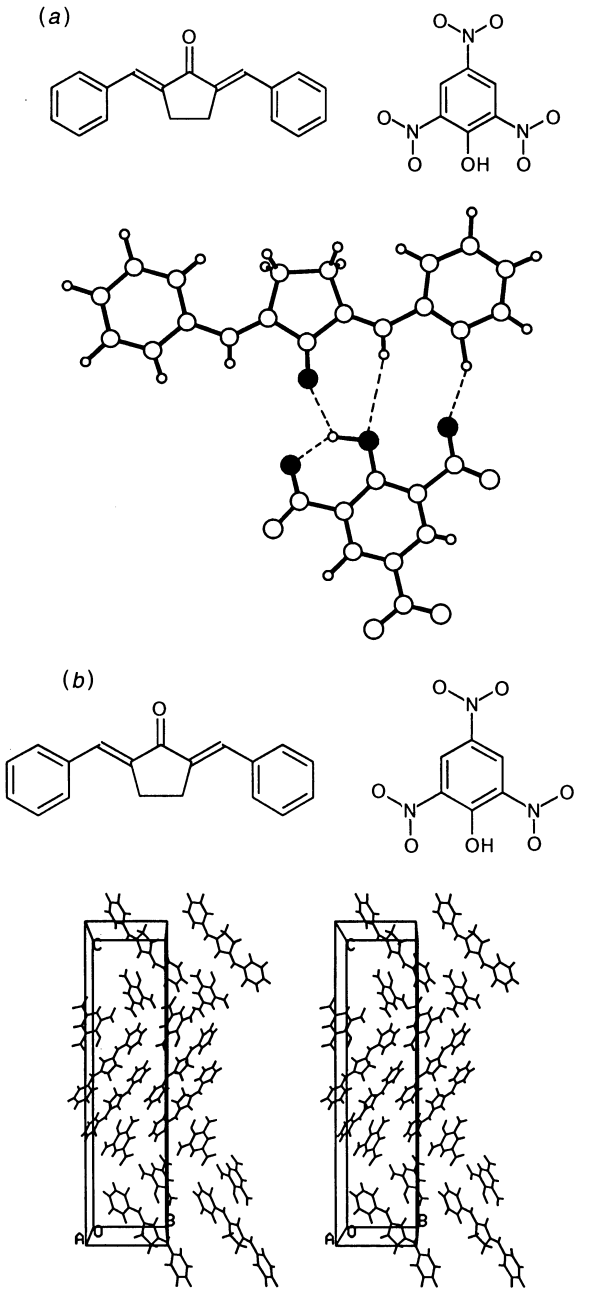

Fig. 4 (*a*) Crystal structure of complex **3f** (**1b**:**2c** in 1:1 ratio) to show the supermolecule that involves one intermolecular O–H , O and two C–H , O hydrogen bonds (oxygen atoms are shaded). (*b*) Packing diagram of the crystal structure of complex **3f**. Note the herringbone and stacking interactions.

189, 159, 44 and 18 crystal structures present for synthons **III**, **IV**, **VIIIa** and **VIIIb**, respectively.

Synthon **III** is present 205 times in 189 crystal structures. Fig. 8(*a*) is the scattergram of C(7) , O(1) *versus* C(3) , O(6) distances and it shows the centrosymmetric nature of **III**. The off-diagonal points are from structures that have two molecules in the asymmetric unit, in other words these interactions occur between symmetry independent molecules. Fig. 8(*b*) is the scattergram of C–H , O angle *versus* C , O distances for **III**.

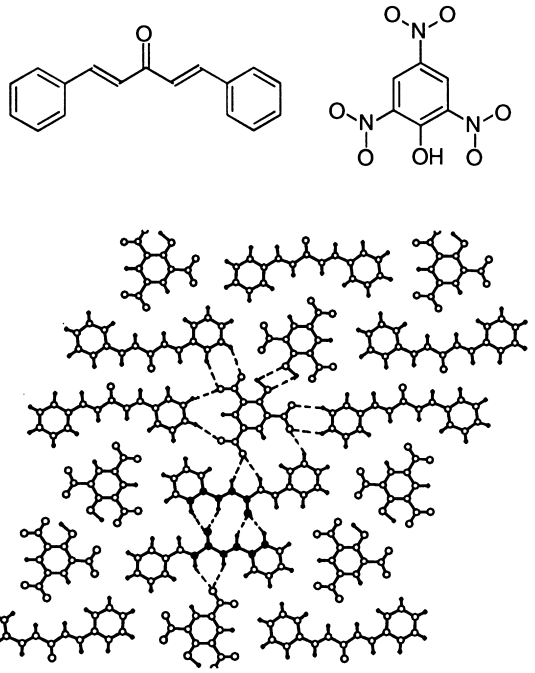

Fig. 5 Packing diagram of the crystal structure of complex **3g** (**1a**:**2c** in 1:1 ratio) to show the dimers of molecules **1a** and **2c** which are formed by C–H , O hydrogen bonded pattern **VIIIa** and O–H , O tandem hydrogen bonds, respectively.

From this plot it can be seen that many of the C–H , O hydrogen bonds are clustered in the strong hydrogen bonds region, *i.e.* in a C , O range of 3.35 to 3.65 Å and a C–H , O range of 155–175°.

There are 173 hits in 159 crystal structures for synthon **IV**. Fig. 9(*a*) is the scattergram of C(9) , O(1) *versus* C(4) , O(6) and indicates the centrosymmetric nature of **IV**. Fig. 9(*b*) is the scattergram of C–H , O angles *versus* C , O distances in **IV**. Here the C–H , O hydrogen bonds are clustered between the C , O distance of 3.25 to 3.55 Å and C–H , O angle of 140 to 160°.

Halogen to nitro oxygen atom contacts are well known and have been used in the design of target crystal structures.[25] A total of 19 crystal structures is present in the CSD for *ortho*-substituted chloro–nitro aromatics and if O , Cl distances only in the range 2.8 to 4.0 Å were considered, 17 of these were found to contain **VII**, indicating robustness of this synthon. There is a total 82 hits from 17 crystal structures for the alternate O , Cl interaction displayed in synthon **IX**. That the number of hits per structure is higher than expected is an artefact of the unsymmetrical O , Cl interaction **IXa** being a subset of the larger synthon **IXb**. From the scattergram of Cl(10) , O(1) *versus* Cl(5) , O(6) distances (Fig. 10), it is clear that the O , Cl interactions exist as symmetrical **VII** and unsymmetrical **IX** variations.

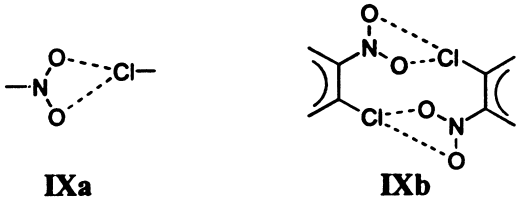

IXa **IXb**

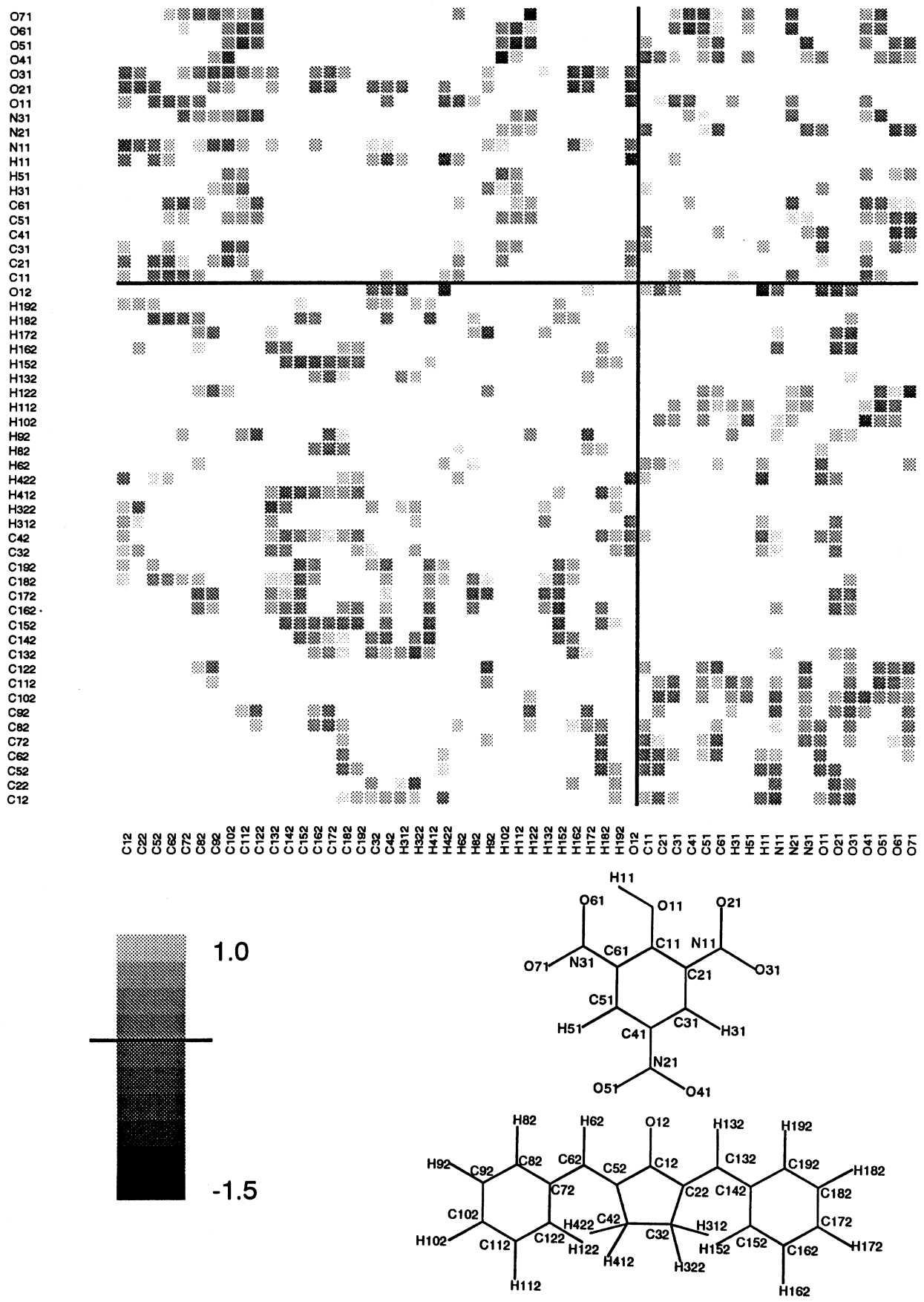

Fig. 6 NIPMAT plots of complexes (*a*) **3f** and (*b*) **3g**. Note that there are more dark grey squares in the upper left and lower right rectangles in (*b*) when compared with (*a*). This indicates stronger and more numerous C–H , O hydrogen bonds and stacking interactions in **3g** compared to **3f**.

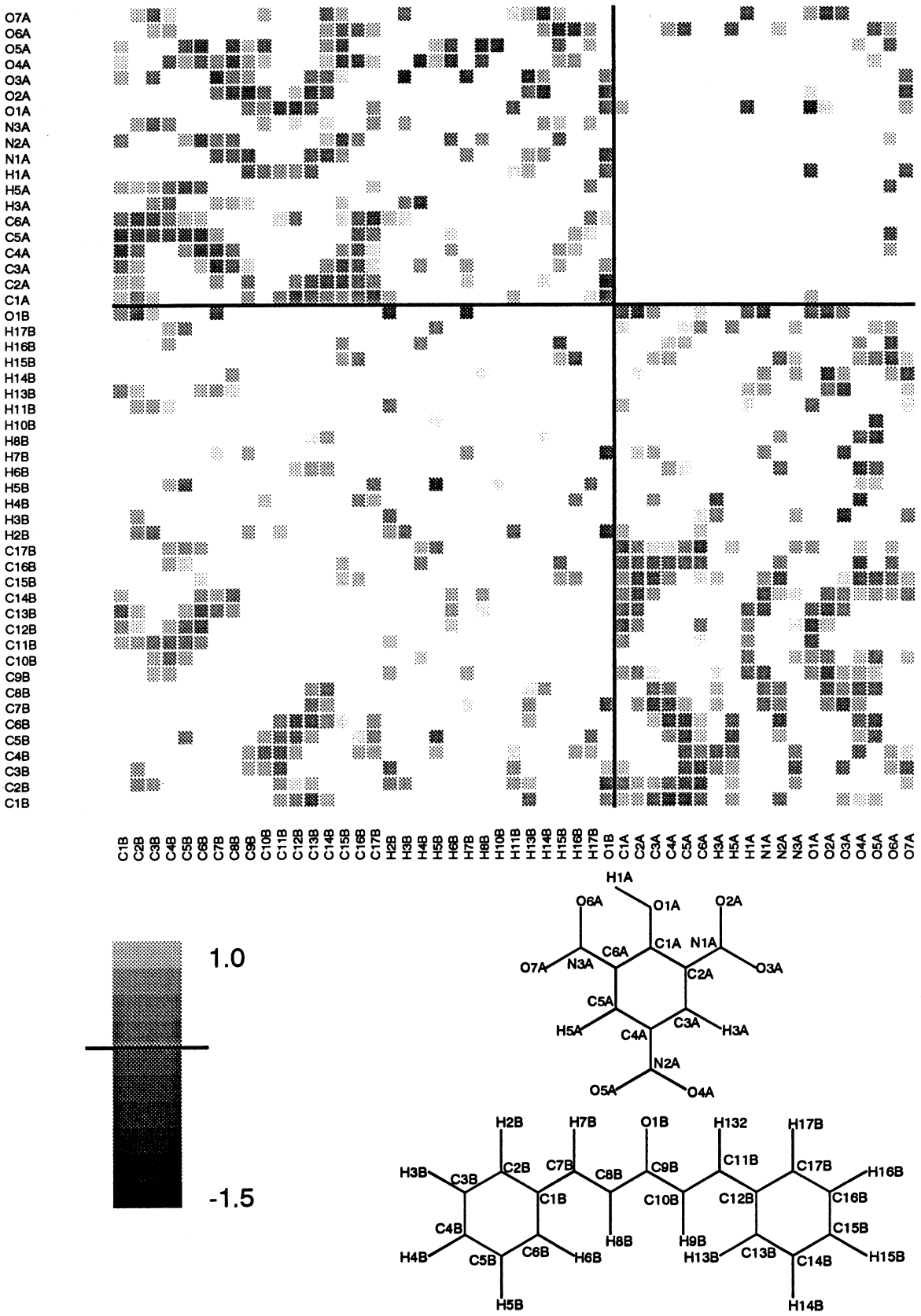

Fig. 6 *(continued).*

Motif **VIIIa** occurs in the molecular complex **3g** and was found 47 times in 44 crystal structures, whereas **VIIIb** was found 18 times in 18 crystal structures. Fig. 11(*a*) is the scattergram of C(15) , O(1) *versus* C(7) , O(9) and shows the centrosymmetric nature of **VIIIa**. Fig. 11(*b*) is the scattergram of C , O distances *versus* C–H , O angles. Open circles represent the C–H , O motifs of **VIIIa** and filled circles represent the C–H , O motifs of **VIIIb**. The C–H , O hydrogen bonds and angles of **VIIIa** are clustered between 3.35 and 3.50 Å and 145 and 155°, and for **VIIIb** they are clustered in the C , O range of 3.15 and 3.35 Å and C–H , O angle range of 135 and 145°. These distance and angle distributions indicate

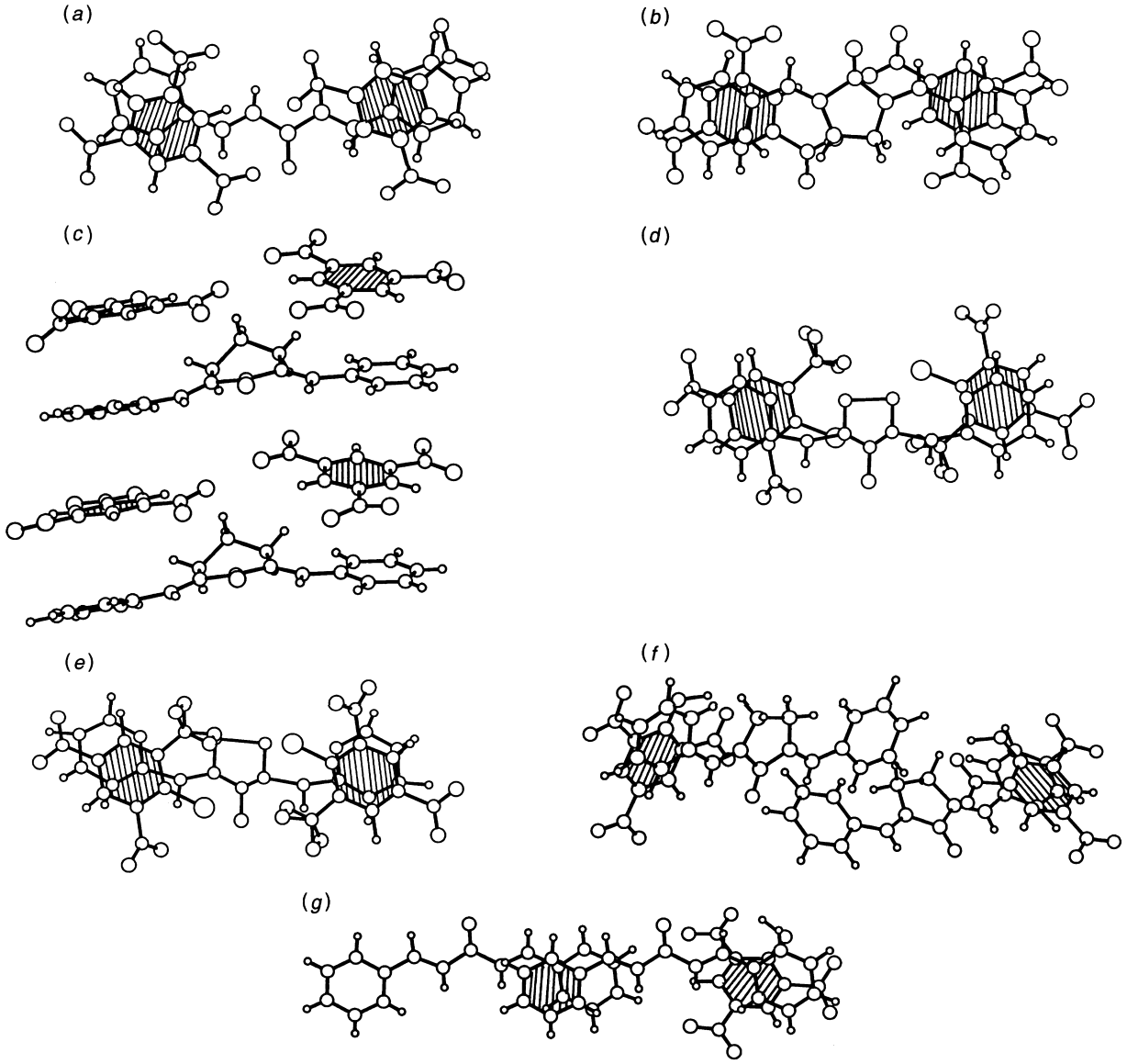

Fig. 7 Stacking interactions of complexes (*a*) **3a**, (*b*) **3b**, (*c*) **3c**, (*d*) **3d**, (*e*) **3e**, (*f*) **3f** and (*g*) **3g**. The phenyl rings of trinitrobenzene derivatives are shaded for clarity.

that many of the C–H , O motifs involved in **VIIIb** are shorter but less linear compared to the hydrogen bonds in synthon **VIIIa**. When Fig. 8(*b*) and 9(*b*) are compared with Fig. 11(*b*) it is clear that the C–H , O bonds involved in synthon **VIIIa,b** are less linear than the bonds in synthons **I** and **III**.

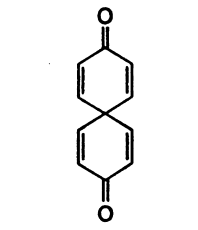

4

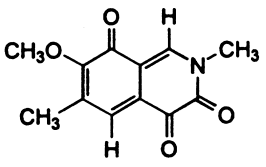

5

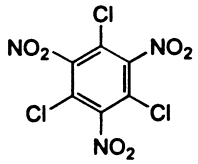

6

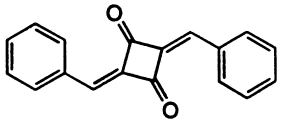

7

Supramolecular synthons III, IV, VII and VIII in crystal engineering

We now discuss a few occurrences of the synthons **III**, **IV**, **VII** and **VIII** to highlight different structural aspects. For this exercise, we have chosen molecules **4–7**. Synthon **III** is the C–H , O counterpart of the N–H , O hydrogen bonded recognition motif found in *cis*-amides. The crystal structure of benzoquinone is composed of synthon **III** which gives it a sheet-like structure. In **4**, the two quinonoid halves of the molecule are tetrahedrally disposed because of the spiro ring junction. In the crystal structure of **4** (Fig. 12), there are two symmetry-independent molecules and these form a ribbon pattern constituted with successive synthons **III**. Only one of the two quinonoid halves of any molecule participates in this pattern and four distinct C , O distances result because two symmetry-independent molecules are involved.[26] The C–H , O dimeric motif and the zig-zag chain arrangement of molecules of **4** resemble the structure found in secondary amides. The crystal structure of **5** (Fig. 13) shows the expected linear chain with synthon **IV**.[27]

The crystal structure of **6** (Fig. 14) is interesting as it maintains the three-fold symmetry with the three nitro groups nearly perpendicular to the plane of the phenyl rings.[28] This arrangement leads to the formation of a rosette-like structure

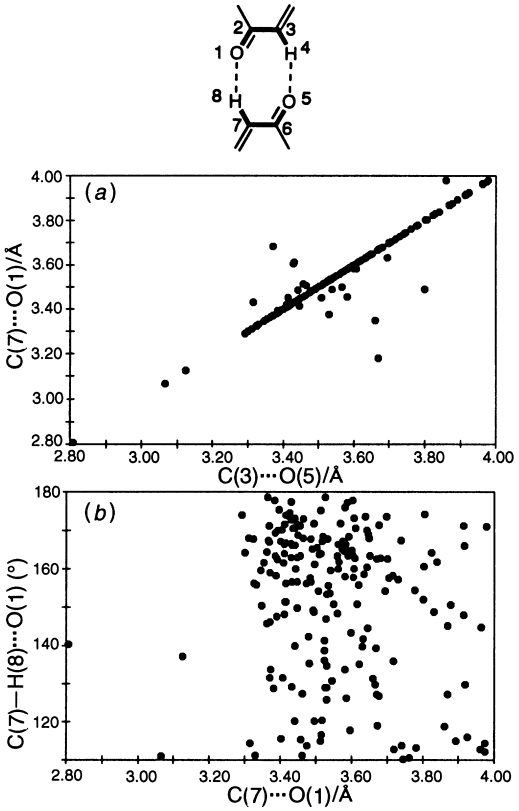

Fig. 8 (*a*) Scatter plot of C , O distances to show the centrosymmetric nature of synthon **III**. (*b*) Scatter plot of C , O distances *versus* C–H , O angles in synthon **III**. Notice that the points are clustered in the C , O range 3.4–3.6 Å and C–H , O range 155–175°.

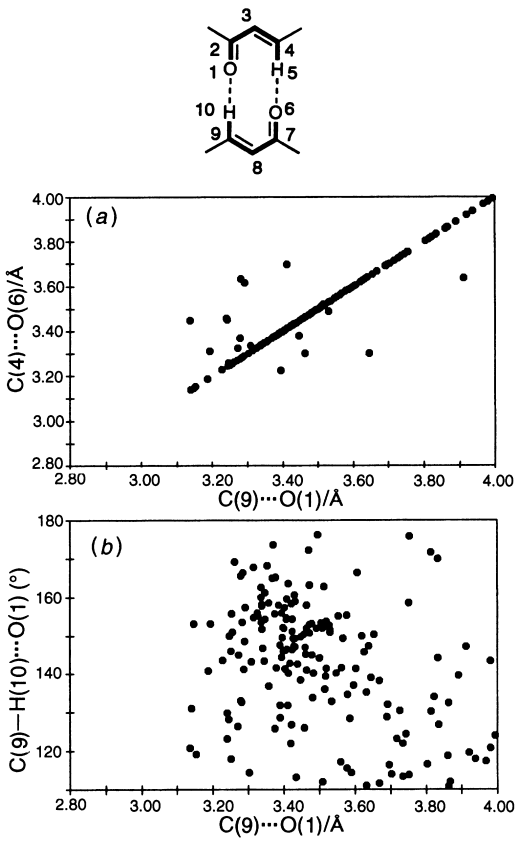

Fig. 9 (*a*) Scatter plot of C , O distances to show the centrosymmetric nature of synthon **IV**. (*b*) Scatter plot of C , O distances *versus* C–H , O angles in synthon **IV**. Notice that the points are clustered in the C , O range 3.25–3.55 Å and in the C–H , O range 140–160°.

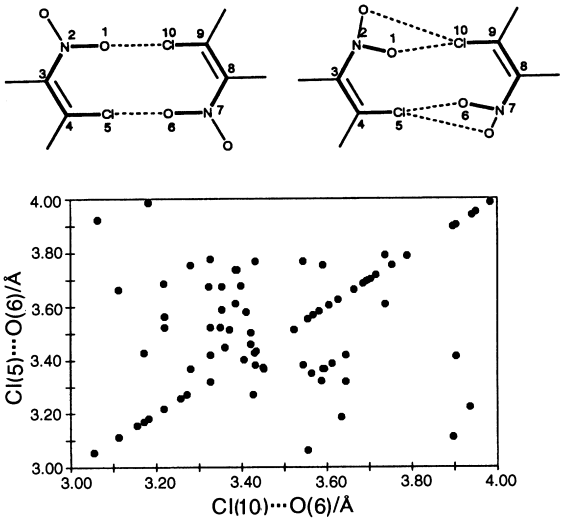

Fig. 10 Scatter plot of Cl(10) , O(1) *versus* Cl(5) , O(6) distances. Notice the centrosymmetric nature of synthons **VII** and **IXb**.

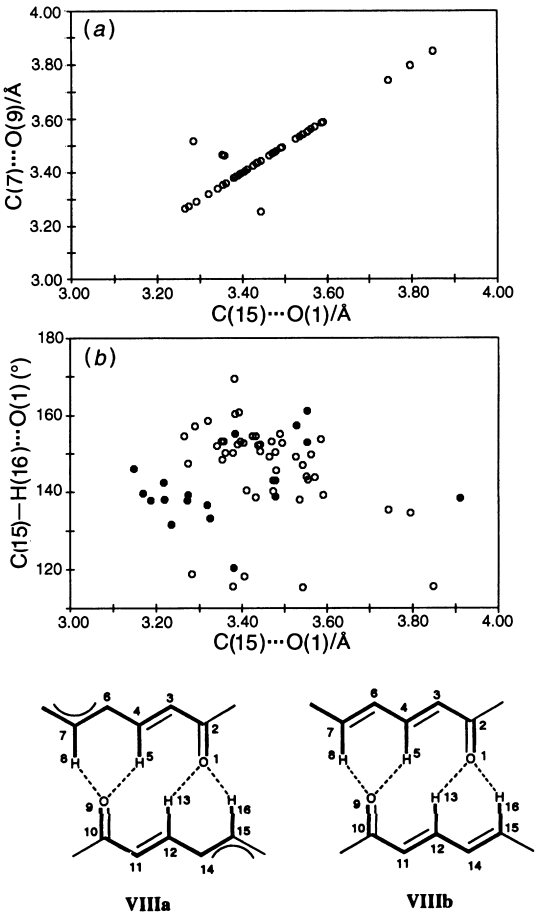

Fig. 11 (*a*) Scatter plot of C(7) , O(9) and C(15) , O(1) distances to show the centrosymmetric nature of synthon **VIIIa**. (*b*) Scatter plot of C , O distances versus C–H , O angles in synthons **VIIIa** and **VIIIb**. Open circles represent the C–H , O hydrogen bonds of synthon **VIIIa** and closed circles represent the bonds in **VIIIb**

with synthon **VII**. The crystal structure of **7** (Fig. 15) contains two molecular components and leads to the anticipated chain structure through C–H , O hydrogen bonds as in synthon **VIII**.[29] These studies suggest that one can utilise **III**, **IV**, **VII** and **VIII** as supramolecular synthons in crystal engineering experiments.

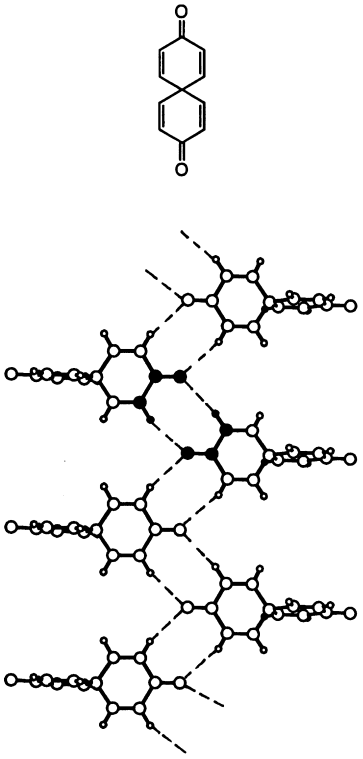

Fig. 12 Crystal structure of **4** (SPUNDD20) to show the zig-zag chain of molecules linked by C–H , O hydrogen bonded synthon **III**

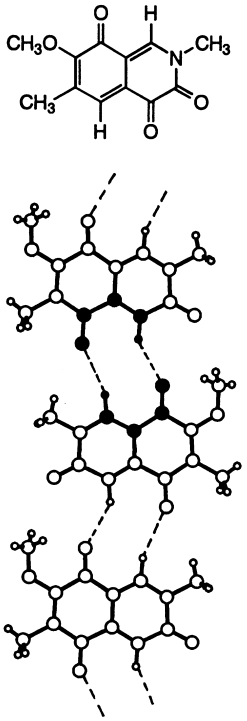

Fig. 13 Crystal structure of **5** (MIMOSA10) to show the linear chain of molecules linked by synthon **IV**

Conclusions

This work shows that C–H , O hydrogen bonds can be profitably utilised to design robust three-point supramolecular synthons. The C–H , O hydrogen bonds involved in multi-point synthons are stronger than the other isolated C–H , O hydrogen bonds in the same and related structures. The presence of strong hydrogen bonding functional groups usually influences C–H , O bonded recognition, but if the strong

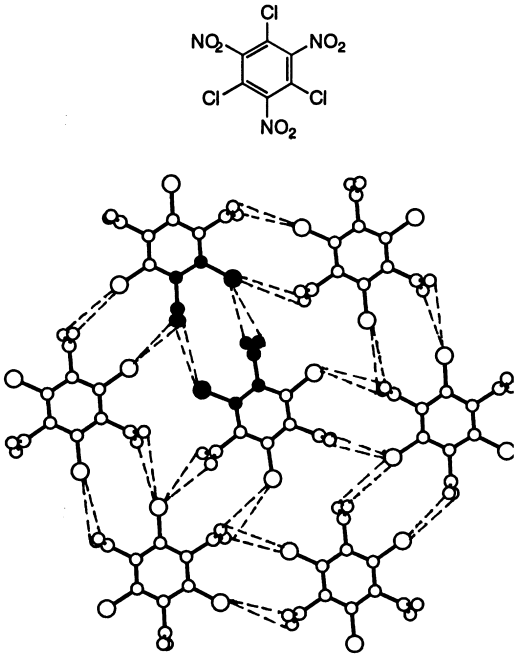

Fig. 14 Crystal structure of **6** (WANMON) to show the hexagonal network of molecules linked through O , Cl interactions of synthon **VII**

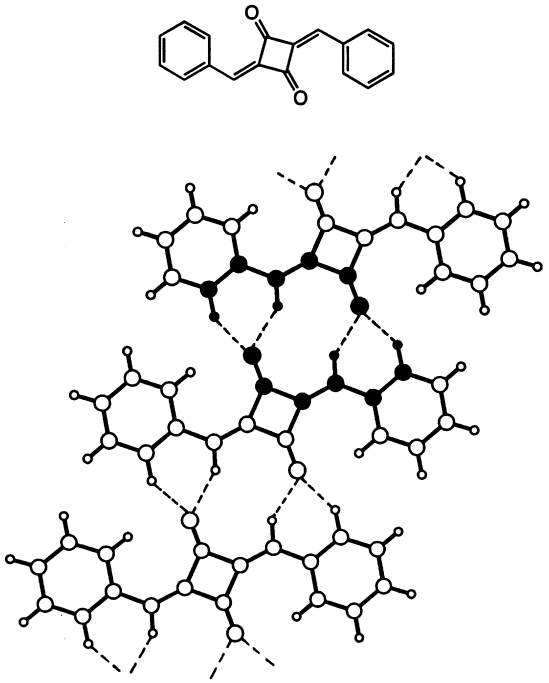

Fig. 15 Crystal structure of **7** (BERGAG) to show the linear arrangement of molecules linked through C–H , O hydrogen bonded synthon **VIIIa**

hydrogen bonds are optimised, the recognition through the weak interactions would be just as effective. Furthermore, the retroanalysis of a supramolecular synthon leads to complementary molecules which assemble in a predictable fashion and form the target motif. Such an approach to the construction of molecular assemblies is analogous to the synthesis of complex molecules from simpler substrates.

Here we have discussed the formation of the C–H , O hydrogen bonded synthon **I** where donors and acceptors are arranged in alternate fashion (ADA : DAD). The related AAD : DDA supramolecular synthon made up of stronger N–H , O and O–H , O hydrogen bonds has been identified recently in the crystal structure of 2′-deoxycytidine

hemidihydrogen phosphate.[30] Such observations lead to the idea that it should also be possible to design related AAA : DDD and AAD : DDA supramolecular synthons with C–H , O hydrogen bonds. Finally, this work also shows that p–p interactions are important in determining the stoichiometry of molecular components and in turn in governing crystal packing.

Financial assistance from the University Grants Commission (K.B.), Department of Science and Technology, Project SP/S1/G19/94 (G.R.D. and A.N.) and Grant CA-10925 from the National Institutes of Health (C.J.C. and H.L.C.) is gratefully acknowledged.

References

1 (*a*) See the organic solid state chemistry special issue of *Chem. Mater*., 1994, **6**, 1087 (ed. M. D. Ward and M. D. Hollingsworth); (*b*) See the nanostructured materials special issue of *Chem. Mater*., 1996, **8**, 1571 (ed. T. Bein and G. D. Stucky).
2 J.-M. Lehn, *Supramolecular Chemistry: Concepts and Perspectives*, VCH, Weinheim, 1995.
3 J. D. Dunitz, in *Perspectives in Supramolecular Chemistry: The Crystal as a Supramolecular Entity*, ed. G. R. Desiraju, Wiley, Chichester, 1996, vol. 2, pp. 1–32.
4 G. R. Desiraju, *Angew. Chem., Int. Ed. Engl*., 1995, **34**, 2311.
5 (*a*) G. R. Desiraju, in *Perspectives in Supramolecular Chemistry: The Crystal as a Supramolecular Entity*, ed. G. R. Desiraju, Wiley, Chichester, 1996, vol. 2, pp. 31–61; (*b*) G. R. Desiraju, in *Comprehensive Supramolecular Chemistry*, ed. D. D. MacNicol, F. Toda and R. Bishop, Pergamon, Oxford, 1996, vol. 6, pp. 1–16.
6 (*a*) J. A. R. P. Sarma and G. R. Desiraju, *Acc. Chem. Res*., 1986, **19**, 222; (*b*) G. R. Desiraju, *Acc. Chem. Res*., 1991, **24**, 290; (*c*) G. R. Desiraju, *Acc. Chem. Res*., 1996, **29**, 441; (*d*) D. S. Reddy, B. S. Goud, K. Panneerselvam and G. R. Desiraju, *J. Chem. Soc., Chem. Commun*., 1993, **663**; (*e*) L. Shimoni, H. L. Carrell, J. P. Glusker and M. M. Coombs, *J. Am. Chem. Soc*., 1994, **116**, 8162; (*f*) D. Braga, F. Grepioni, K. Biradha and G. R. Desiraju, *J. Chem. Soc., Dalton Trans*., 1996, 3925.
7 (*a*) V. R. Pedireddi and G. R. Desiraju, *J. Chem. Soc., Chem., Commun*., 1992, 988; (*b*) T. Steiner and W. Saenger, *J. Am. Chem. Soc*., 1993, **115**, 4540; (*c*) T. Steiner and W. Saenger, *J. Am. Chem. Soc*., 1992, **114**, 10146.
8 (*a*) V. R. Thalladi, K. Panneerselvam, C. J. Carrell, H. L. Carrell and G. R. Desiraju, *J. Chem. Soc., Chem. Commun*., 1995, 341; (*b*) C. V. K. Sharma and G. R. Desiraju, *J. Chem. Soc., Perkin Trans. 2*, 1994, 2345; (*c*) T. Suzuki, H. Fujii and T. Miyashi, *J. Org. Chem*., 1992, **57**, 6744.
9 D. Braga, F. Grepioni, K. Biradha, V. R. Pedireddi and G. R. Desiraju, *J. Am. Chem. Soc*., 1995, **117**, 3156.
10 A preliminary account of this work has appeared: K. Biradha, C. V. K. Sharma, K. Panneerselvam, L. Shimoni, H. L. Carrell, D. E. Zacharias and G. R. Desiraju, *J. Chem. Soc., Chem. Commun*., 1993, 1473.
11 (*a*) H. D. William, H. D. Rosenblatt, W. G. B. Rosenblatt and L. C. Clifford, *J. Chem. Eng. Data*, 1975, **20**, 202; (*b*) A. I. Vogel, *A Text-Book of Practical Organic Chemistry*, 3rd edn., English Language Book Society, 1975, p. 758; (*c*) A. I. Vogel, *A Text-Book of Practical Organic Chemistry*, 3rd edn., E.L.B.S, 1975, p. 965.
12 E. T. Borrows, J. C. Clayton, B. A. Hems and A. G. Long, *J. Chem. Soc*., 1949, S190.
13 G. R. Desiraju and K. V. R. Kishan, *Indian J. Chem., Sect. B*, 1988, **27**, 953.
14 W. Ried and F. Anthofer, *Angew. Chem*., 1953, **65**, 601.
15 G. M. Sheldrick, SHELXS86, in *Crystallographic Computing 3*, ed. G. M. Sheldrick, C. Kruger and R. Goddard, Oxford University Press, Oxford, UK, 1985, pp. 175–189.
16 G. M. Sheldrick, SHELXL, An Integrated System for Solving, Refining and Displaying Crystal Structures from Diffraction Data, University of Göttingen, Germany, 1993.
17 F. H. Allen, J. E. Davies, J. J. Galloy, O. Johnson, O. Kennard, C. F. Macrae and D. G. Watson, *J. Chem. Inf. Comput. Sci*., 1991, **31**, 204.
18 S. K. Kearsley and G. R. Desiraju, *Proc. R. Soc. London, Ser. A*, 1985, **397**, 157.
19 H. Nagata, Y. In, M. Doi and T. Ishida, *Acta Crystallogr., Sect. B*, 1995, **51**, 1051.
20 V. Agafonov, P. Dubois, F. Moussa, J. M. Cense and S. Toscani, *J. Chem. Soc., Perkin Trans. 2*, 1994, 2007.
21 G. A. Jeffrey and W. Saenger, *Hydrogen Bonding in Biological Structures*, Springer-Verlag, Berlin, 1991, p. 24.
22 C. A. Hunter and J. K. M. Sanders, *J. Am. Chem. Soc*., 1990, **112**, 5525.
23 R. Foster, *Organic Charge-Transfer Complexes*, Academic Press, London, 1969, p. 113.
24 (*a*) M. Harmata and C.L. Barnes, *J. Am. Chem. Soc*., 1990, **112**, 5655; (*b*) M. Harmata, C. L. Barnes, S. R. Karra and S. Elahmad, *J. Am. Chem. Soc*., 1994, **116**, 8392.
25 (*a*) V. R. Thalladi, B. S. Goud, V. J. Hoy, F. H. Allen, J. A. K. Howard and G. R. Desiraju, *Chem. Commun*., 1996, 401; (*b*) F. H. Allen, B. S. Goud, V. J. Hoy, J. A. K. Howard and G. R. Desiraju, *J. Chem. Soc. Chem. Commun*., 1994, 2729.
26 D. L. Cullen, B. Hass, D. G. Klunk, T. V. Willoughby, C. N. Morimoto, E. F. M. Junior, G. Farges and A. Dreiding, *Acta Crystallogr., Sect. B*, 1976, **32**, 555.
27 T. Hata, H. Fukumi, S. Sato, K. Aiba and C. Tamura, *Acta. Crystallogr., Sect. B*, 1978, **34**, 2899.
28 F. Gerard, A. Hardy and A. Becuwe, *Acta Crystallogr., Sect. C*, 1993, **49**, 1215.
29 B. M. Gatehouse, *Cryst. Struct. Commun*., 1982, **11**, 365.
30 M. Jaskólski, M. Gdaniec, M. Gilski, M. Alejska and M. D. Bratek-Wiewiórowska, *J. Biomol. Struct. Dyn*., 1994, **11**, 1287.

Paper 6/07106F; *Received* 18*th October*, 1996